ISSN 1727-7337 (print)
ISSN 2663-2217 (online)

UDC 621.45.022.5

doi: 10.32620/aktt.2026.4.04

Nijat ABDULLA

National Aviation Academy, Baku, Azerbaijan

NUMERICAL TREATMENT OF POLYMORPHIC SPECIES IN MULTIPHASE CHEMICAL-EQUILIBRIUM SOLVERS

*This article presents a phase-stability criterion for treating polymorphic condensed species in high-fidelity chemical equilibrium modeling. The **aim** of the article is to prevent polymorph locking, invalid coefficient usage, and unstable phase switching in Gibbs free-energy minimization when composition-identical solid phases exhibit small free-energy differences near solid-solid transition boundaries. The **methods** are rooted in identifying compositionally identical condensed candidates, separating true polymorphic families from solid-liquid phase-transition cases, and inferring solid-solid transition temperatures from thermochemical-database interval adjacency using a dedicated phase-transition detection procedure. The stable polymorph is selected based on the current temperature relative to the inferred boundary, while preserving elemental composition and stoichiometric constraints. If no transition temperature can be reliably inferred, a temperature-validity check is applied, and out-of-range polymorphs are replaced with admissible counterparts of identical composition. This phase-admissibility layer is coupled with the condensed active-set stability test, ensuring that only thermodynamically stabilizing condensed phases remain in the equilibrium solution. The **scientific novelty** of the article lies in the explicit integration of polymorph phase-stability logic into KKT-based multiphase combustion-equilibrium iterations and active-set decision procedures. The proposed criterion regularizes solid-solid switching, prevents thermodynamic-data leakage outside valid polynomial intervals, and improves convergence robustness near phase-boundary regions. Benchmark temperature-sweep cases involving Cr_2O_3 polymorphs demonstrate stable temperature-dependent phase selection and agreement with NASA CEA at the property level, with an average relative error of approximately 0.05%. The results show that explicit phase-stability criteria provide a physically consistent and robust foundation for modeling polymorphic species in multiphase chemical equilibrium calculations.*

Keywords: *chemical equilibrium modeling; polymorphic species; phase stability; Gibbs free-energy minimization; condensed phases; solid-solid phase transition; active-set method; thermochemical database; high-temperature combustion; KKT-based equilibrium solver*

1. Introduction

High-fidelity chemical equilibrium modeling is a fundamental tool in the preliminary and refined design of aerospace propulsion systems. In jet and rocket engines, the equilibrium state of combustion products determines flame temperature, molecular weight, specific heat, throat sonic conditions, nozzle expansion, thermal loading, and overall performance [1, 2, 3]. Under severe pressure-temperature conditions, dissociation, minor-species formation, condensed phases, and strong thermodynamic-property variations must be treated explicitly [4, 5, 6]. Therefore, Gibbs free-energy minimization remains a central method for predicting reacting-mixture composition and properties under prescribed thermodynamic constraints [7, 8, 9, 10].

Classical equilibrium programs, including NASA CEA and related thermochemical solvers, have long provided a reliable basis for combustion analysis [11, 12, 13]. They determine equilibrium states through minimization of the total thermodynamic potential of a multicomponent system under elemental-conservation and phase admissibility constraints. For gas-dominated combustion, this approach is usually robust for predicting flame temperature, product composition, and mixture properties. In systems involving condensed species, phase boundaries, triple-point neighborhoods, or multiple crystalline forms of the same compound, however, the solution also depends on correctly identifying the thermodynamically admissible phase at the current temperature and pressure.

Condensed-phase treatment is critical in high-temperature combustion systems containing metal species, oxidized particles, solid residues, or condensed intermediates. The solver must determine whether a condensed species should be activated, removed, or replaced by another phase with the same composition. While this is simple when Gibbs free-energy differences are large, near phase-transition boundaries competing phases may have nearly equal potentials. As a result, small errors in temperature, polynomial evaluation, or active-set selection can cause incorrect phase selection, oscillations, or use of coefficients outside their valid temperature range.

Among condensed-phase difficulties in combustion-equilibrium modeling, polymorphism is especially

important and often underestimated. It denotes the existence of multiple solid phases of the same compound, each with a distinct crystal structure and thermodynamic-property representation [14, 15]. In constrained Gibbs-minimization, polymorphs are not different chemical substances but competing condensed forms with identical elemental composition and different Gibbs free-energy functions. Therefore, the solver must explicitly select the phase thermodynamically stable at the current state. Otherwise, it may lock onto an initially active polymorph even after the temperature crosses the transition region.

The difficulty increases because solid-solid transitions usually occur over narrow temperature intervals. Although Gibbs free energy remains the governing potential, its derivatives may change abruptly, weakening the smoothness assumptions of Newton-type solvers. This can make the Jacobian ill-conditioned, alter the condensed-species active set suddenly, and cause stagnation or nonphysical phase switching [16, 17, 18, 19]. Similar behavior occurs near vapor-liquid, solid-liquid, and triple-point conditions, where the phase assemblage is highly sensitive to small thermodynamic perturbations [17, 20]. These effects directly affect the predicted species distribution, enthalpy, entropy, and heat-release characteristics of the equilibrium mixture.

Accurate phase-stability treatment depends on reliable and internally consistent thermochemical data. Equilibrium calculations require temperature-dependent heat capacity, enthalpy, entropy, and Gibbs free energy for all candidate species [21, 22], which are commonly represented in combustion solvers by NASA-type polynomial coefficients over finite temperature intervals [23]. For polymorphic condensed species, each phase may have its own validity range, and the transition boundary may be inferred from interval adjacency or overlap. Therefore, evaluating a polynomial outside its admissible range can introduce an artificial thermodynamic preference and cause incorrect phase selection. A consistent polymorph-selection method must therefore combine Gibbs-potential comparison, temperature-validity checking, and database-based phase-boundary detection.

In high-pressure combustion systems, real-gas behavior, non-ideal interactions, and strong composition-property coupling introduce additional modeling challenges [24, 25, 26]. Although ideal-gas assumptions remain useful in many propulsion calculations, condensed phases introduce inequality constraints and phase-appearance conditions that must be solved together with the equilibrium equations. Active-set logic is therefore effective: condensed candidates are activated only when their chemical-potential condition indicates admissibility, whereas unstable phases are removed. For polymorphic species, however, this logic must also identify composition-identical solid candidates and prevent simultaneous or incorrect selection of incompatible phase forms.

The present article addresses the formulation of phase-stability criteria for polymorphic species in high-temperature chemical equilibrium modeling. Polymorphic condensed species are identified by identical elemental composition and treated as alternative phase representations rather than independent chemical products. After detecting a polymorphic family, the solver attempts to infer a transition temperature from the thermochemical database. When this boundary is available, the stable polymorph is selected according to the current temperature; otherwise, temperature-admissibility logic replaces an out-of-range polymorph with a valid composition-identical alternative. This procedure prevents thermodynamic data leakage, reduces artificial phase locking, and improves the physical consistency of the equilibrium solution. By addressing these issues, the work supports the development of more reliable multiphase equilibrium solvers for combustion systems involving complex condensed species, high-temperature dissociation, and phase-sensitive thermodynamic behavior [27, 28, 29].

2. Chemical Equilibrium Model

The equilibrium composition is obtained by minimizing Gibbs free-energy G subject to elemental conservation and nonnegative species amounts:

$$\sum_{j=1}^{\eta_s} \mathbf{A}_{ij}\mathbf{N}_j - \mathbf{B}_i^\circ = 0 \tag{1}$$

In Eq. 1 $\mathbf{A}_{ij}$ is the elemental-composition matrix, $\mathbf{B}_i^\circ$ is the assigned elemental abundance, $\mathbf{N}_j$ is the species moles and η_s is the total number of species. Introducing Lagrange multipliers gives

$$\mathcal{L} = \left\langle \mu_j, \mathbf{N}_j \right\rangle + \sum_{i=1}^{\zeta} \lambda_j \left(\mathbf{B}_i - \sum_{j=1}^{\eta_s} \mathbf{A}_{ij}\mathbf{N}_j \right) \tag{2}$$

The equilibrium condition $\delta\mathcal{L} = 0$ yields

$$\mu_j + \sum_{i=1}^{\zeta} \lambda_i \mathbf{A}_{ij} = 0 \tag{3}$$

The chemical potential is pressure-sensitive for gaseous species but weakly dependent on pressure for condensed phases, which are nearly incompressible [30, 31]. Therefore, the chemical potential is written as

$$\mu_j = \begin{cases} \mu_j^\circ + \phi_\circ \ln\left(p\mathbf{N}_j n^{-1}\right) & 1 \le j \in \mathbb{Z} \le \eta_g \\ \mu_j^\circ & 1 \le j \in \mathbb{Z} \le \eta_c \end{cases} \tag{4}$$

ISSN 1727-7337 (print)
ISSN 2663-2217 (online)

where η_g and η_c are the numbers of gaseous and condensed species, respectively. Eq.'s 1 and 3 define the equilibrium composition for assigned pressure and temperature, $p = p_\circ$ and $T = T_\circ$. For constant pressure and enthalpy problems (PH), the additional condition is $h = h_\circ$, with $h = \sum_j \mathbf{N}_j \mathbf{H}_j^\circ$. For constant pressure and entropy problems (PS), the additional condition is $s = s_\circ$, where $s = \sum_j \mathbf{N}_j \mathbf{S}_j$, where $\mathbf{S}_j$, representing the entropy of species j, can be expanded as

$$\mathbf{S}_j = \begin{cases} \mathbf{S}_j^\circ - R_\circ \ln\left(p \mathbf{N}_j n^{-1}\right) & 1 \le j \in \mathbb{Z} \le \eta_g \\ \mathbf{S}_j^\circ & 1 \le j \in \mathbb{Z} \le \eta_c \end{cases} \quad (5)$$

The resulting nonlinear system is solved iteratively by linearizing the equilibrium and conservation equations. The unknown corrections are $\Delta \ln \mathbf{N}_j$ for gaseous species, $\Delta \mathbf{N}_j$ for condensed species, $\Delta \ln n$, the nondimensional multipliers $\mathbf{\Pi}_i = \lambda_i \left[R_\circ T\right]^{-1}$, and, when required, $\Delta \ln T$. These variables define a coupled Newton-type update for composition, mixture size, elemental potentials, and temperature. For constant pressure, the linearized equilibrium equations are:

$$\Delta \ln \mathbf{N}_j - \sum_{i=1}^{\zeta} \mathbf{A}_{ij} \mathbf{\Pi}_i - \Delta \ln n - \frac{\mathbf{H}_j^\circ \Delta \ln T}{\phi_\circ} = -\frac{\mu_j}{\phi_\circ} \quad (6)$$

for gaseous species, and

$$-\phi_\circ \sum_{i=1}^{\zeta} \mathbf{A}_{ij} \mathbf{\Pi}_i - \mathbf{H}_j^\circ \Delta \ln T = -\mu_j \quad (7)$$

for condensed species. The elemental-balance and Dalton constraints are

$$\sum_{j=1}^{\eta_g} \mathbf{A}_{kj} \mathbf{N}_j \Delta \ln \mathbf{N}_j + \sum_{j=1}^{\eta_c} \mathbf{A}_{kj} \Delta \mathbf{N}_j = \mathbf{B}_k^\circ - \mathbf{B}_k \quad (8)$$

and

$$\sum_{j=1}^{\eta_g} \mathbf{N}_j \left(\Delta \ln \mathbf{N}_j + 1\right) = n\left(\Delta \ln n + 1\right) \quad (9)$$

Eq.'s 6-9 form the base system for the constant-pressure and constant-temperature problem. The PT formulation treats pressure and temperature as prescribed, while PH and PS introduce temperature as an unknown and impose enthalpy or entropy closure, respectively, as

$$H\left(T, p, \mathbf{N}\right) = H_\circ \quad \text{and} \quad S\left(T, p, \mathbf{N}\right) = S_\circ \quad (10)$$

To solve the equilibrium composition system, the Descent Newton-Raphson (DNR) method is applied. It combines Newton curvature information with a controlled descent strategy. For a nonlinear objective function $f\left(\mathbf{X}\right)$, the classical Newton direction is written as

$$\mathbf{P}_k^{(N)} = -\nabla^2 f\left(\mathbf{X}_k\right)^{-1} \nabla f\left(\mathbf{X}_k\right) \quad (11)$$

where $\nabla f\left(\mathbf{X}_k\right)$ and $\nabla^2 f\left(\mathbf{X}_k\right)$ are the gradient and Hessian at the current iteration. Although this direction gives rapid quadratic convergence near a well-conditioned minimum, it may fail when the Hessian is indefinite, singular, or poorly conditioned. To improve robustness, the DNR method introduces damping, regularization, or line-search control so that each iteration follows a descent direction and avoids unstable updates. The general update is expressed as

$$\mathbf{X}_{k+1} = \mathbf{X}_k + \alpha_k \mathbf{P}_k \quad (12)$$

where $\alpha_k \in (0,1]$ is chosen to ensure sufficient decrease of the objective function. Away from the solution, DNR behaves as a stabilized descent scheme, while near convergence it approaches the classical Newton-Raphson form. This makes it suitable for nonlinear and ill-conditioned engineering problems. Tab. 1 summarizes the comparison between the classical and descent Newton-Raphson methods.

Table 1

Comparison of Newton-Raphson Methods

Component	Classical Newton-Raphson	Descent Newton-Raphson (Adaptive Step Size)
Step Direction	$-\mathbf{H}^{-1}\nabla f$	Same
Step Size	$\alpha = 1$	$\alpha_k \in (0,1]$ via Line Search
Descent Guarantee	Not Guaranteed	Guaranteed with Proper α Value
Global Robustness	Limited	Improved
Local Convergence	Quadratic	Quadratic
Applicability	Best Near Minimum	Effective Both Near and Far from Minimum

In addition, the DNR method is widely used in large-scale numerical optimization, machine-learning algorithms, and engineering-design problems, where both convergence speed and stability are crucial. By combining the curvature-based precision of Newton's method with the robustness of line-search techniques, this approach strikes a balance between local accuracy and global convergence. The inclusion of an adaptive step size ensures that each iteration yields a decrease in the objective function, making the method more reliable in practice, especially when the initial guess is far from the optimum or the Hessian is not positive definite.

3. Computational Framework

Robust phase-boundary handling is essential for extending a gas-only equilibrium solver to propulsion-grade condensed-regime calculations. In the present framework, composition-identical condensed phases are detected, transition boundaries are inferred from database validity intervals, and PH iterations use modified logarithmic updates with boundary snapping and coexistence tolerance. These procedures ensure that phase activation and deactivation remain thermodynamically consistent even near sharp transition regions, where small temperature changes can otherwise trigger unstable phase switching. As a result, repeated phase-boundary crossing is suppressed, coefficient validity is preserved, and the nonlinear equilibrium solve remains stable, as summarized in Tab. 2.

Table 2

Core Transition Utilities and Their Thermodynamic Meaning

Utility/Quantity	Implementation Role	Thermodynamic Interpretation
meltingPoint	Returns T_m for Solid-Liquid Pair	Proxy for Solid-Liquid Coexistence Boundary (Melting Temperature)
phaseTransitionPoint	Returns $T_{\alpha\rightleftharpoons\beta}$	Solid-Solid Transition Inferred from Database Adjacency and Bounds
triplePointTolerance	Defines Coexistence Band Around Boundary	Numerical Tolerance for Triple Point/Coexistence Activation

The solver detects solid-liquid coexistence by searching for condensed candidates with identical elemental atom vectors and treating them as alternative phase representations of the same chemical formula. When both `Solid` and `Liquid` labels are present within such a composition-identical group, the transition is classified as a melting boundary. The corresponding melting temperature, T_m, is then evaluated using `meltingPoint`, which scans the matching database records and infers the boundary from the liquid lower-temperature limit or the solid upper-temperature limit. This approach is consistent with the NASA polynomial validity segmentation, where phase changes are represented indirectly through adjacent temperature intervals rather than through an explicit phase-diagram table. Thus, the solver identifies solid-liquid boundaries directly from the thermochemical database, as summarized in Tab. 3. As a result, the phase-transition logic remains fully database-driven and does not require additional empirical `meltingPoint` input.

Table 3

Decision Logic for Solid-Liquid Coexistence Near Melting Point

Step	Input Data	Computational Action
Phase Differentiation	Species Phase Labels	Detect Presence of Solid and Liquid Representations
Coexistence Classification	Matched Species Set	Classify System as Potential Melting Boundary
Melting Temperature Inference	Temperature Intervals (Database)	Compute T_m via Lower Liquid Bound or Upper Solid Bound

The refinement over a naive approach lies in **how the solver reacts when the iterated temperature approaches** T_m. Rather than allowing temperature updates to oscillate across the boundary and repeatedly flip the active phase, **the algorithm introduces a tolerance band** defined by `triplePointTolerance`. When $|T - T_m|$ is larger than this tolerance, the solver enforces a single-phase selection rule: if $T < T_m$, liquid candidates are replaced by solid entries of identical composition; if $T > T_m$, the inverse replacement is applied. This replacement does not change stoichiometry, and therefore preserves the feasibility of elemental constraints, but it changes the thermodynamic functions ($\mu^\circ(T)$, $H^\circ(T)$, etc.) in a proper way. If $|T - T_m|$ is less than `triplePointTolerance`, the solver declares a triple-point coexistence regime by setting `triplePointDetector` to

`True`, activates the second phase explicitly by adding it to the condensed set with an initial amount of zero, and snaps the iterated temperature to T_m. This snapping is a critical stabilization step: it transforms a numerically stiff crossing of a discontinuous admissibility change into a **well-defined coexistence point at which both phases are admissible**. This prevents artificial phase flip-flop and keeps the active-set structure consistent during the Newton update. Consequently, the discontinuous phase-selection problem is converted into a controlled coexistence treatment without violating thermodynamic admissibility.

A central practical question in triple-point and phase-boundary handling is the selection of the coexistence tolerance ε, implemented as `triplePointTolerance` (see [32]). This parameter defines the temperature band within which the solver (i) treats two composition-identical phases as simultaneously admissible, (ii) activates the coexisting phase explicitly, and (iii) snaps the iterate to the boundary temperature, e.g., $T \rightleftharpoons T_m$ (see Fig. 1).

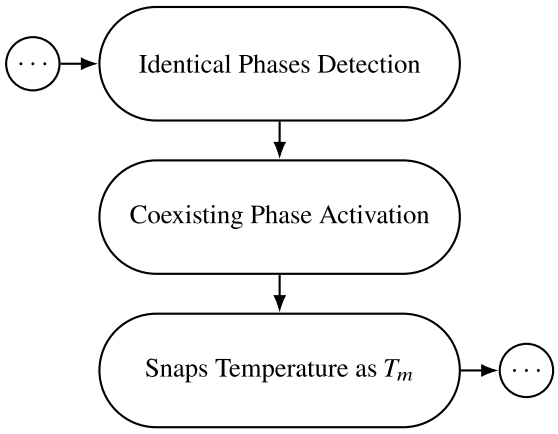

Fig. 1. Phase Change Handling Workflow at Melting Boundary

If ε is too small, the solver may repeatedly cross the phase boundary, causing phase flip-flop, data-validity loss, and slow convergence. If ε is too large, coexistence may be activated too far from the boundary, giving unphysical phase freedom and biased compositions. Therefore, ε must be chosen as a regularization tolerance based on database temperature intervals, local property curvature, and the PH/PS temperature-correction scale.

Here, ε is treated as **a temperature-space capture radius** around database-inferred phase boundaries. These boundaries correspond to melting points for solid-liquid transitions and polymorphic transition points for solid-solid cases. Near T_b, discontinuous polynomial segmentation and condensed-phase active-set switching make the Newton update sensitive to the sign of $T - T_b$. The coexistence tolerance stabilizes this behavior by stopping repeated boundary chasing and solving the equilibrium at the boundary with both phases admissible.

A suitable ε must both capture the boundary and avoid excessive phase activation. If $\Delta T^{(k)}$ is the undamped temperature correction and α is the damping factor, the effective step is $\alpha\left|\Delta T^{(k)}\right|$, or $\alpha\left|\Delta \ln T^{(k)}\right|T$ for multiplicative temperature updates. Therefore, ε should be larger than the characteristic damped temperature step near the boundary, but smaller than the temperature range over which the competing phase descriptions become thermodynamically distinct:

$$\varepsilon \geq \eta\alpha\left|\Delta T\right|^{\circ} \tag{13}$$

Here, $1 \leq \eta \in \mathbb{R} \leq 3$ is a safety factor, and $\left|\Delta T\right|^{\circ}$ is the typical temperature-correction magnitude observed during condensed-phase activation or swapping. To avoid premature coexistence, ε must also remain small relative to the narrowest relevant database temperature interval and within a locally linear thermodynamic-property range:

$$\varepsilon \ll \Delta T_{\text{int,min}} \quad \text{and} \quad \varepsilon \ll \left|\mu^{\circ}(T)\nabla_T \mu^{\circ}\right|_{T=T_b} \tag{14}$$

The first bound ties ε to database segmentation; the second ties it to the local scale of variation of the standard chemical potential, and by extension h and s, near the boundary.

In practice, the solver uses a global tolerance, `triplePointTolerance`, for simplicity and reproducibility. Its purpose is to prevent phase flip-flop when composition-identical condensed phases alternate while T repeatedly crosses the inferred boundary T_b. If the tolerance is too small, boundary snapping is not activated and convergence may slow due to repeated active-set reconstruction. If it is too large, snapping may occur prematurely and artificially constrain the thermodynamic state. Thus, `triplePointTolerance` is chosen as a compromise between reliable boundary capture and thermodynamic localization.

4. Findings and Discussion

Polymorphic and solid-solid transitions are examined using a constant-pressure and constant-temperature model temperature-sweep benchmark for metal-containing multiphase systems. The test stresses condensed-phase stability and polymorph selection, where small temperature changes can switch the stable solid form without changing pressure or mixture ratio. Results are compared directly with NASA CEA to isolate differences caused by phase-selection logic.

Table 4

Polymorphic Transition Verification Cases

Case ID	Inputs to Simulate (Fuel/Oxidizer, Temperatures, O/F, Pressure, Constraint)
PPT-1, PPT-2, PPT-3, PPT-4	Fuel: Liquid CH_4 (95%, 111.643 K), Cr (5%, 298.15 K), Li (5%, 298.15 K); Oxidizer: Liquid O_2 at 90.17 K; O/F=5.00; 200 bar; 250, 308, 312, and 350 K

Tab. 4 fixes pressure and mixture ratio while sweeping temperature across a range sensitive to solid-solid transitions. Chromium was included as a condensed test species because it provides a sensitive and physically consistent case for verifying phase-boundary handling in the solver. In the considered temperature range, chromium has thermodynamic-property representations that change across a narrow solid-state transition region, while the chemical composition of the condensed species remains identical. Therefore, any change in the calculated equilibrium state is not caused by a change in elemental abundance, pressure, or mixture ratio, but by the solver's ability to select the thermodynamically admissible condensed form. The relatively small chromium fraction is sufficient to activate the relevant condensed-phase candidates without dominating the methane–oxygen combustion system, making it suitable for isolating numerical behavior near polymorphic or solid-state transition boundaries. Consequently, Cr serves as a controlled verification species for testing phase selection, database-interval validity, and active-set stability in comparison with NASA CEA.

The cases are first reduced to the fixed elemental abundance vector $\mathbf{B}_i^\circ$; any changes with T then reflect phase selection and are compared to NASA CEA.

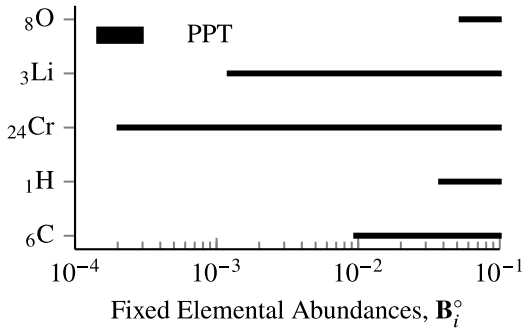

Fig. 2. PPT: Elementary Composition

Fig. 2 shows the fixed elemental abundance vector $\mathbf{B}_i^\circ$ for the PPT mixture (C, H, Cr, Li, O). Since pressure and mixture ratio are constant across the sweep for different problems, $\mathbf{B}_i^\circ$ is unchanged and any differences are temperature driven phase effects.

Table 5

Polymorphic Cases: Molecular Weight and Enthalpy

Property	Value	Unit
Molecular Weight	27.2081	g/mol
Enthalpy	-917.3943	kJ/(kg·K)

Tab. 5 summarizes the reactant-side mixture molecular weight and enthalpy for the PPT benchmark. Because the reactant composition is kept identical throughout the temperature sweep for all case studies, both quantities remain unchanged across all PPT cases. They therefore define a fixed inlet thermochemical reference state, allowing the observed differences in the results to be attributed primarily to temperature-dependent polymorphic phase selection rather than to changes in mixture composition.

After the elemental composition of the propellant mixture is determined, and the corresponding mixture molecular weight and enthalpy values are evaluated, the convergence behavior of the equilibrium solution can be analyzed through the iteration history of the regularization parameter and the Lagrange multipliers. The study of the variation of these two parameters is quite enough to make sure that the results are stably converged. The variation of the regularization parameter indicates how strongly the Newton correction is damped during the early and near-boundary stages of the solution, while the evolution of the Lagrange multipliers reflects the stabilization of the elemental-balance constraints. Therefore, these quantities provide useful diagnostic measures for assessing whether the nonlinear equilibrium system approaches a stable and physically consistent solution. A smooth approach of these parameters toward nearly constant values indicates that the active set and thermodynamic state have become consistent. Conversely, persistent oscillations or abrupt jumps may indicate phase-boundary switching, excessive damping, or an ill-conditioned equilibrium update.

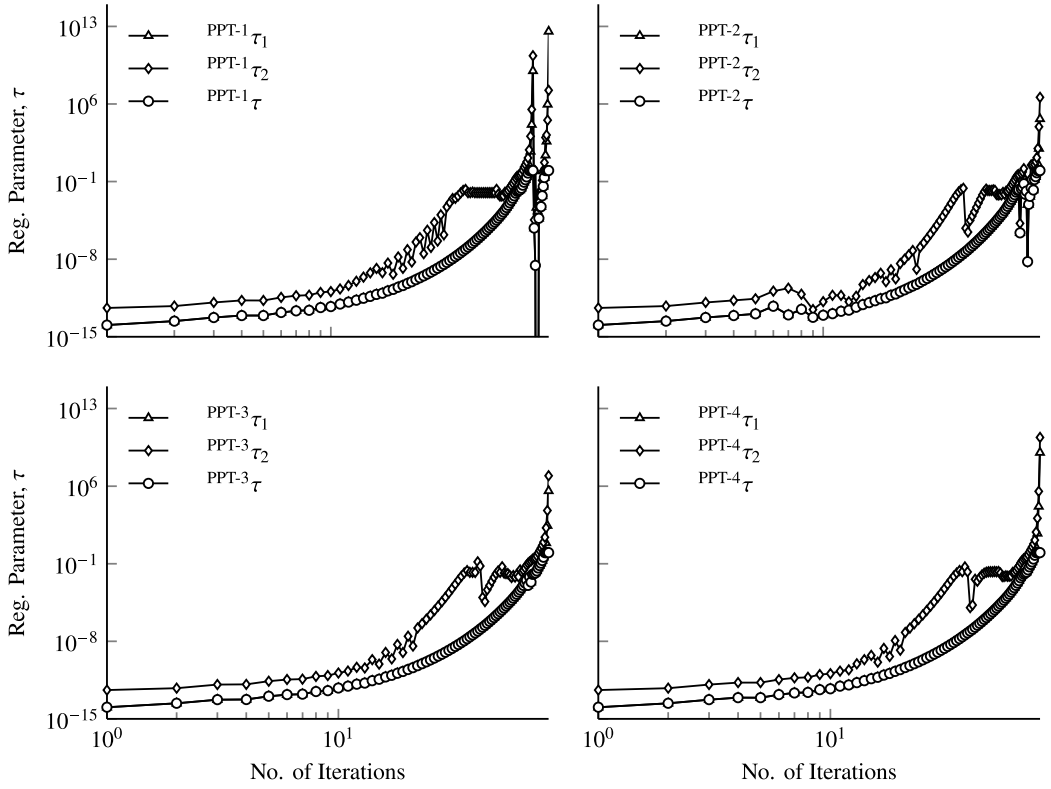

Fig. 3. Polymorphic Transition Cases: Regularization Parameter

Fig. 3 shows the evolution of the regularization parameter τ for the PPT temperature-sweep cases. In all four benchmarks, $\tau < 1$ during the early iterations indicates damping of the update step while the solver stabilizes the condensed-phase selection and approaches the equilibrium state. As the residuals decrease, τ approaches unity, showing that the corrections become well behaved and that full steps are gradually accepted. The consistent relaxation of τ across the temperature sweep indicates stable numerical treatment of polymorphic phase selection despite the changes in the preferred solid form with temperature.

The behavior of the regularization parameter confirms that the solver does not rely on **abrupt or uncontrolled Newton corrections** near the polymorphic transition region. Instead, the parameter remains below unity when the equilibrium problem is locally ill-conditioned, thereby reducing the correction magnitude and preventing **excessive movement across competing phase boundaries**. Once the active condensed phase becomes consistent with the thermodynamic state and the residual structure becomes smoother, the regularization parameter increases toward unity. This behavior demonstrates the intended transition from a damped, stabilized iteration regime to a nearly full Newton-type correction regime, which is essential for maintaining both robustness and convergence efficiency in phase-sensitive equilibrium calculations.

This gradual increase also indicates that the solver avoids premature acceptance of large updates while the active set is still uncertain. In the PPT cases, such behavior is particularly important because small temperature changes can alter the preferred chromium solid form and temporarily flatten the local Gibbs free-energy landscape. Therefore, the observed regularization trend supports the conclusion that the proposed algorithm can manage polymorphic sensitivity **without sacrificing convergence stability**.

With the regularization behavior established, the variation of the elemental Lagrange multipliers can now be examined in more detail. Their iteration histories provide an additional view of how the elemental balance constraints are enforced throughout the solution process as the system approaches the final equilibrium state. In the present benchmark, these multipliers are especially useful for tracking how the constraint enforcement adapts as the stable condensed form changes with temperature and different polymorphs become thermodynamically preferred.

Fig. 4 shows the iteration histories of the elemental Lagrange corrections for the PPT temperature-sweep cases. In all four benchmarks, the multipliers undergo their main adjustment during the early iterations and then stabilize as the solver approaches equilibrium, indicating the consistent enforcement of elemental balance across the full set of elements. The differences between cases reflect the change in thermodynamic state with temperature and the corresponding shift in the stable condensed-

phase selection. In particular, the variation of the multipliers across the temperature sweep is consistent with the fact that different solid forms become thermodynamically preferred in different temperature intervals, so the Lagrange corrections adapt to the changing polymorphic equilibrium state while remaining numerically well-behaved.

The behavior of the elemental Lagrange corrections $\mathbf{\Pi}_i$ shows that the elemental-balance constraints remain controlled throughout the polymorphic transition process. During the initial iterations, relatively larger corrections are required because the solver is simultaneously adjusting the gas-phase composition, condensed-phase activity, and elemental constraint multipliers. This early adjustment stage reflects the coupled nature of the equilibrium problem, where changes in phase selection directly influence the distribution of elements among admissible species. As the active phase set becomes thermodynamically consistent, the corrections decrease and approach a stable pattern, indicating that the constrained minimization problem is being solved without violating elemental conservation.

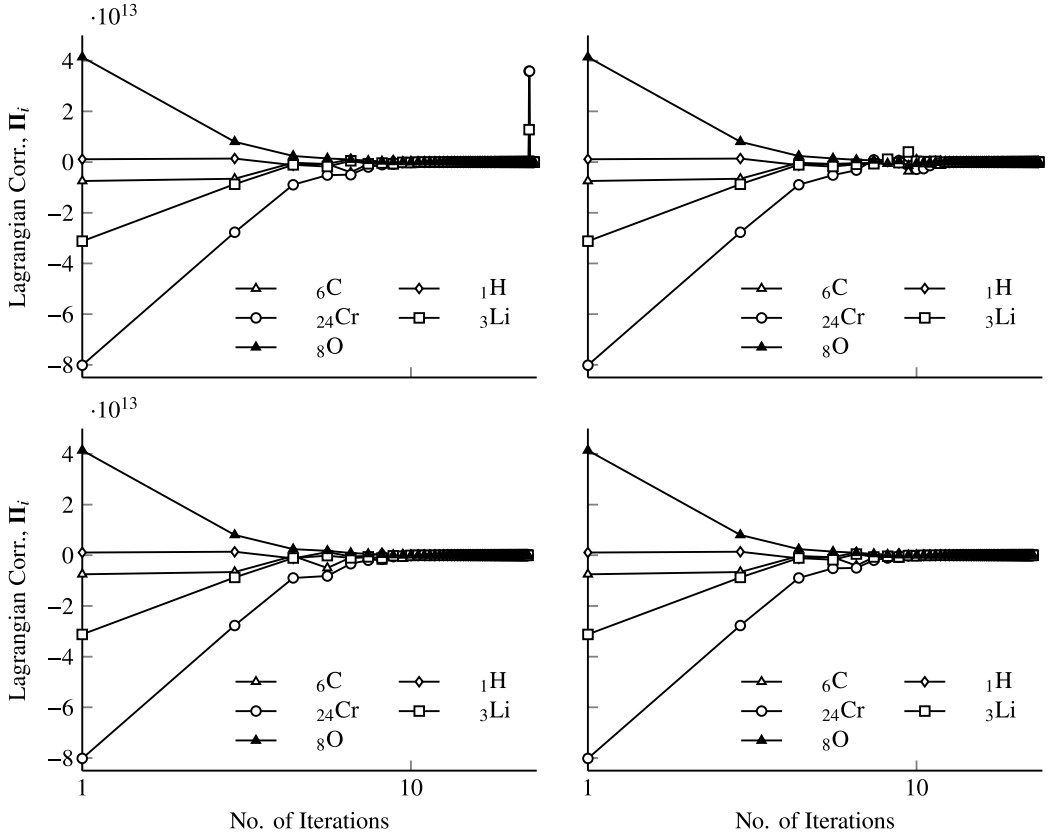

Fig. 4. Polymorphic Transition Cases: Lagrangian Corrections

This stabilization is important because $\mathbf{\Pi}_i$ directly reflects how the Gibbs minimization procedure enforces the elemental abundance vector $\mathbf{B}_i^{\circ}$. If polymorphic switching caused numerical instability, the Lagrange corrections would exhibit persistent oscillations, abrupt divergence, or repeated readjustment between competing condensed forms. Instead, their bounded and convergent behavior confirms that the proposed active-set treatment preserves the coupling between phase selection and elemental balance. Therefore, the observed $\mathbf{\Pi}_i$ histories support the robustness of the solver in phase-sensitive equilibrium calculations, particularly when composition-identical condensed candidates compete over narrow temperature intervals.

Fig. 5 shows the convergence of the mixture moles per unit mass n for the PPT temperature sweep at fixed pressure and mixture ratio. In all cases, n evolves during the initial iterations as the solver rescales the total mixture amount consistently with the developing equilibrium composition, including the activation and stabilization of condensed phases in a metal-bearing system. As the KKT residuals decay and the active condensed set stabilizes, the n trajectories collapse to a common converged value ($n \cong 0.0157$), indicating that the total-moles normalization is satisfied consistently across the sweep. The near overlap of the iteration curves further implies that, over the selected temperature range, the total mixture scaling is only weakly sensitive to temperature once the elemental inventory and pressure are fixed, even though the detailed phase partitioning may change. This behavior

ISSN 1727-7337 (print)
ISSN 2663-2217 (online)

provides an additional convergence indicator complementary to τ and $\mathbf{\Pi}_i$, confirming that the solver reaches a self-consistent equilibrium state for each temperature without nonphysical oscillations in the total-moles.

With convergence established in τ, $\mathbf{\Pi}_i$, and n for all PPT cases, the equilibrium state is fully specified at each temperature. The resulting outputs can therefore be used to examine the temperature-dependent stability of polymorphic condensed species, including when a given solid form becomes active, when it is replaced by an alternative polymorph, and how these transitions redistribute mass between competing condensed phases.

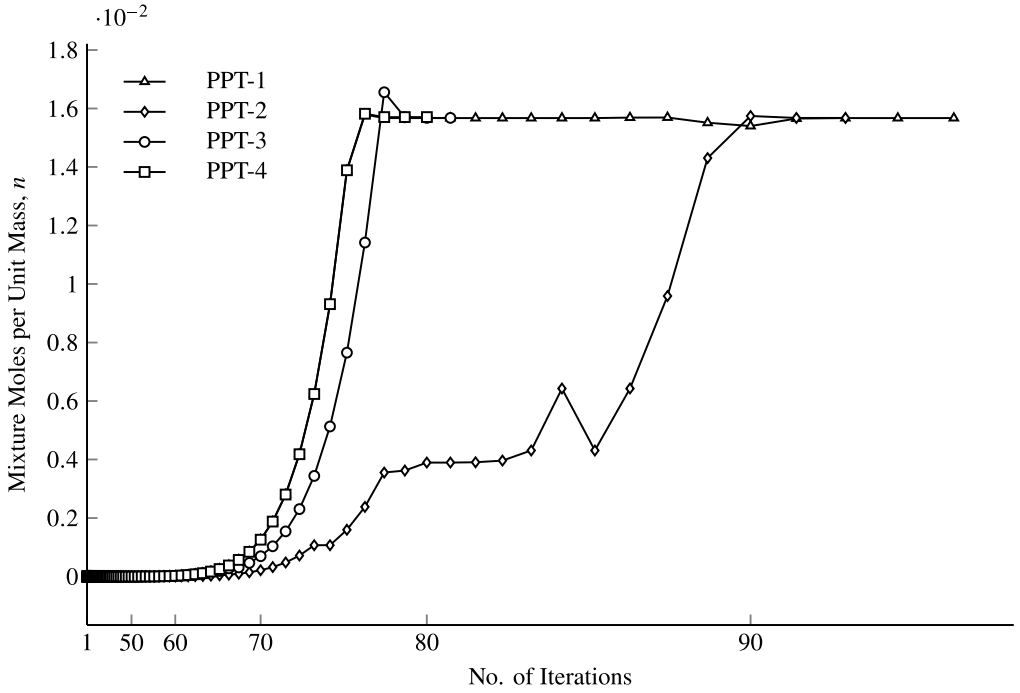

Fig. 5. Polymorphic Transition Cases: Mixture Moles per Unit Mass

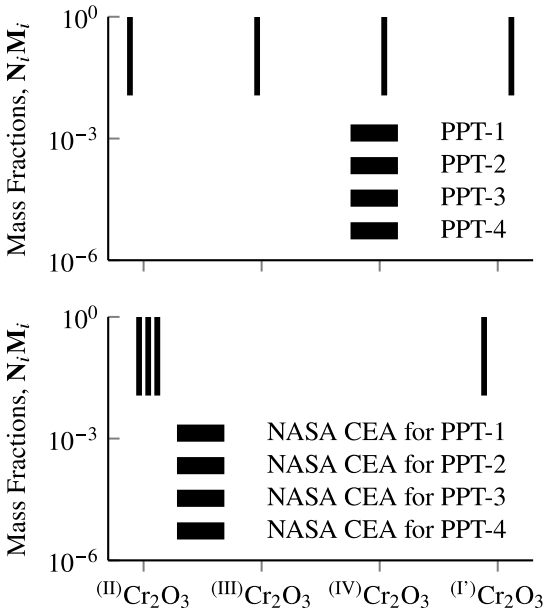

Fig. 6. Polymorphic Transition Cases: Species Mass Fractions

In present benchmarks, the primary polymorphic candidate is Cr_2O_3, and its activation and solid-solid transition behavior across the temperature sweep are analyzed. Fig. 6 summarizes the temperature-dependent polymorph selection for Cr_2O_3 across the PPT sweep by reporting the equilibrium mass fraction associated with each solid form. The present implementation exhibits consistent phase selection: each temperature point activates a single Cr_2O_3 polymorph as the thermodynamically stable condensed form, with the same total Cr_2O_3 mass fraction (0.01218) preserved while the identity of the stable polymorph changes across the sweep. In contrast, the NASA CEA results in the same figure indicate that the reference solution may identify the $^{(I')}Cr_2O_3$ entry as the stable form for the PPT-1 condition, but then report $^{(I)}Cr_2O_3$ for the remaining temperatures, **effectively fixing the polymorph selection** rather than transitioning consistently as the stability ordering changes with T. The present solver, on the other hand, avoids this artifact by enforcing **explicit polymorph resolution** during condensed-phase activation and by applying temperature-interval validity checks for adjacent solid entries, ensuring that the active condensed form corresponds to the stable Cr_2O_3 polymorph at each mixture temperature value. Consequently, the observed polymorph switching in the present results reflects controlled, stability-driven solid-

solid transitions rather than a hard-coded or database-order-dependent selection.

Tab. 6 summarizes the mean relative error for the PPT temperature sweep. Across all four cases, the agreement with NASA CEA remains uniformly tight at the property level, with the average deviation staying on the order of 0.05 over 250-350 K. The remaining error is dominated primarily by **the internal-energy convention difference for heterogeneous mixtures**, while the other state and mixture properties exhibit only minor deviations attributable to numerical tolerances and output rounding, rather than to discrepancies in equilibrium phase stability or polymorph selection.

Table 6

Polymorphic Cases: Molecular Weight and Enthalpy

Property	PPT-1–4
Average Relative Error	0.05%

5. Conclusion

The results show that explicit polymorph-stability criteria improve both numerical robustness and thermodynamic consistency in multiphase chemical-equilibrium calculations. By identifying composition-identical condensed species, separating true solid-solid polymorphic transitions from solid-liquid cases, and using thermochemical-database validity intervals, the solver selects the admissible polymorph without relying on external phase-diagram data.

The developed method prevents polymorph locking, invalid coefficient usage, and unstable phase switching near transition boundaries. Coupling this logic with Gibbs free-energy minimization, condensed active-set control, and regularized Newton iterations preserves elemental stoichiometry while maintaining phase validity at the current temperature. The Cr_2O_3 temperature-sweep benchmarks confirm stable convergence, temperature-dependent polymorph selection, and close agreement with NASA CEA, with an average relative error of approximately 0.05%.

Overall, the proposed treatment provides a practical basis for reliable modeling of condensed products, metallic species, and phase-sensitive thermochemical behavior in propulsion-oriented equilibrium solvers, especially where temperature-dependent phase selection can influence mixture properties and downstream engine-performance predictions.

Contributions of author: research concept and design, development of the computational methodology, thermochemical data analysis, implementation of the phase-stability criterion, numerical modeling, verification against NASA CEA, analysis and interpretation of results, writing the article, preparation of figures and tables, and critical revision of the article – **Nijat Abdulla**.

Conflict of Interest

The author declares that there is no conflict of interest in relation to this research, whether financial, personal, authorship-related, or otherwise, that could affect the research, its results, or the conclusions presented in this paper.

Financing

This study was conducted without financial support.

Data Availability

The work has associated data that can be provided upon reasonable request.

Use of Artificial Intelligence

The author confirms that artificial intelligence methods were not used in creating the presented work.

The author has read and agreed to the published version of this manuscript.

References

1. Catana, R. M., Badea, G. P. Experimental analysis on the operating line of two gas turbine engines by testing with different exhaust nozzle geometries, *Energies*, 2023, vol. 16, iss. 15. 20 p. DOI: 10.3390/en16155627

2. Abdulla, N., Abdullayev, P. S. The generalized tensor model for numerical investigation of combustion and flow processes in liquid rocket engine chamber, *Journal of Aeronautics and Space Technologies*, 2023, vol. 16, iss. 1, pp. 15–40. Available at: https://jast.hho.msu.edu.tr/index.php/JAST/article/view/514

3. Abdulla, N. Numerical investigation of combustion equilibrium in thrust chambers of liquid rocket engines. *Proceedings of the 73rd International Astronautical Congress*, Paris, France, 18–22 September 2022. Available at: https://dl.iafastro.directory/event/IAC-2022/paper/68767/

4. Moreno-Pacheco, L.A., Sánchez-López, F., Barbosa-Saldaña, J. G., Martínez-Trinidad, J., Carpinteyro-Pérez, M. A., Wong-Ángel, W., García-León, R.A. Design and numerical analysis of an annular combustion chamber, *Fluids*, 2024, vol. 9, iss. 7. 26 p. DOI: 10.3390/fluids9070161

5. Kulczycki, A., Przysowa, R., Białecki, T., Gawron, B., Jasiński, R., Merkisz, J., Pielecha, I. Empirical modeling of synthetic fuel combustion in a small turbofan, *Energies*, 2024, vol. 17, iss. 11. 19 p. DOI: 10.3390/en17112622

6. Zhu, Y., Wang, S., Wang, K., Liu, Y., Liu, C.,

Liu, F., Yang, J., Mu, Y., Xu, G. A review of ignition characteristics and prediction model of combustor under high-altitude conditions, *Energies*, 2025, vol. 18, iss. 3. 26 p. DOI: 10.3390/en18030527

7. Zhao, W., Yang, X., Wang, J., Zheng, Y. and Zhou, Y. Evaluation of thermodynamic and chemical kinetic models for hypersonic and high-temperature flow simulation, *Applied Sciences*, 2023, vol. 13, iss. 17, 20 p. DOI: 10.3390/app13179991

8. Saccone, G., Marini, M. Chemical kinetic analysis of high-pressure hydrogen ignition and combustion toward green aviation, *Aerospace*, 2024, vol. 11, iss. 2, 17 p. DOI: 10.3390/aerospace11020112

9. Gordon, S., McBride, B. J. *Computer program for calculation of complex chemical equilibrium compositions and applications. Part 1: Analysis*. NASA Reference Publication 1311. Washington, DC: NASA, 1994. Available at: https://ntrs.nasa.gov/citations/19950013764

10. McBride, B. J., Gordon, S. *Computer program for calculation of complex chemical equilibrium compositions and applications II. Users manual and program description*. NASA Reference Publication 1311. Washington, DC: NASA, 1996. Available at: https://ntrs.nasa.gov/citations/19960044559

11. National Aeronautics and Space Administration *Chemical equilibrium with applications*. NASA Glenn Research Center, 2025. Available at: https://www.nasa.gov/glenn/research/chemical-equilibrium-with-applications/

12. *Cantera Developers Cantera: an object-oriented software toolkit for chemical kinetics, thermodynamics, and transport processes*, 2026. Available at: https://cantera.org/

13. *RP Software+Engineering UG Rocket Propulsion Analysis*, 2026. Available at: https://www.rocket-propulsion.com/index.htm

14. Herranz, M., Benito, J., Foteinopoulou, K., Karayiannis, N. C., Laso, M. Polymorph stability and free energy of crystallization of freely-jointed polymers of hard spheres, *Polymers*, 2023, vol. 15, iss. 6. 20 p. DOI: 10.3390/polym15061335

15. Al-Rawe, S. K., Baranov, D., Bronowska, A. K., Cano, C., Carroll, M. A., Waddell, P. G. Polymorphism in N-(3-hydroxyphenyl)-3-methoxybenzamide', *Crystals*, 2024, vol. 14, iss. 12. 13 p. DOI: 10.3390/cryst14121070

16. Kaptay, G. The generalized phase rule, the extended definition of the degree of freedom, the component rule and the seven independent non-compositional state variables: to the 150th anniversary of the phase rule of Gibbs, *Materials*, 2024, vol. 17, iss. 24. 34 p. DOI: 10.3390/ma17246048

17. Chi, Z., Ji, Y., Liu, N., Jiang, T., Liu, X., Zhang, W. Algorithms for solving the equilibrium composition model of arc plasma, *Entropy*, 2025, vol. 27, iss. 1, 24 p. DOI: 10.3390/e27010024

18. Moravvej, Z., Bazargani, Z., Esmaeilzadeh, F. Thermodynamic modeling and optimization of biomass and bio-renewable organic source gasification in supercritical water using Gibbs free energy minimization, *Water*, 2024, vol. 16, iss. 15. 17 p. DOI: 10.3390/w16152123

19. dos Santos Junior, J. M., dos Reis, L. P., Vidotti, A. D. S., de Freitas, A. C. D., Mariano, A. P., Guirardello, R. Thermodynamic modeling of low-temperature Fischer–Tropsch synthesis: a Gibbs free energy minimization study for hydrocarbon production, *Processes*, 2025, vol. 13, iss. 8. 22 p. DOI: 10.3390/pr13082373

20. Lopez-Zamora, S., Escobedo, S. and de Lasa, H. A machine learning approach for phase-split calculations in n-octane/water and PASN/water systems, *Processes*, 2022, vol. 10, iss. 4. 26 p. DOI: 10.3390/pr10040710

21. Bains, W., Petkowski, J. J., Zhan, Z., Seager, S. A data resource for prediction of gas-phase thermodynamic properties of small molecules, *Data*, 2022, vol. 7, iss. 3. 19 p. DOI: 10.3390/data7030033

22. Moreno, D. E., Hargather, C. Z. Thermodynamic properties as a function of temperature of AlMoNbV, NbTaTiV, NbTaTiZr, AlNbTaTiV, HfNbTaTiZr, and MoNbTaVW refractory high-entropy alloys from first-principles calculations, *Solids*, 2023, vol. 4, iss. 4, pp. 327–343. DOI: 10.3390/solids4040021

23. McBride, B. J., Zehe, M. J., Gordon, S. *NASA Glenn coefficients for calculating thermodynamic properties of individual species*. NASA/TP-2002-211556. Cleveland, OH: NASA Glenn Research Center, 2002. Available at: https://ntrs.nasa.gov/citations/20020085330

24. Luo, H., Xin, Q., Yao, C., Li, C., Yang, T., Wu, X., Chahine, R., Xiao, J. Effect of real gas equations on calculation accuracy of thermodynamic state in hydrogen storage tank, *Applied Sciences*, 2025, vol. 15, iss. 20. 13 p. DOI: 10.3390/app152011151

25. Ren, J., Yang, F., Ma, D., Le, G., Zhong, J. Pneumatic performance study of a high pressure ejection device based on real specific energy and specific enthalpy, *Entropy*, 2014, vol. 16, iss. 9, pp. 4801–4817. DOI: 10.3390/e16094801

26. Madana Gopal, J. V., Morgan, R., De Sercey, G., Vogiatzaki, K. Overview of common thermophysical property modelling approaches for cryogenic fluid simulations at supercritical conditions, *Energies*, 2023, vol. 16, iss. 2. 30 p. DOI: 10.3390/en16020885

27. Hosseini, A., Hage, J. L. T., Meijer, K., Offerman, E.,Yang, Y. On the importance of model selection for CFD analysis of high temperature gas-solid reactive flow; case study: post combustion chamber of HIsarna off-gas system, *Processes*, 2023, vol. 11, iss. 3. 38 p. DOI: 10.3390/pr11030839

28. Korukçu, M. Ö. A graphical user interface for calculating exergy destruction for combustion reactions, Processes, 2024, vol. 12, iss. 2. 17 p. DOI: 10.3390/pr12020294

29. Gao, J., Zhang, K., Lyu, W., Zhang, Y., Wang, M., Cheng, Y., Li, A., Chen, X. Molecular dynamics simulation of phase behavior of fluid in confined nanopores, *Processes*, 2025, vol. 13, iss. 2. 13 p. DOI: 10.3390/pr13020506

30. Kocherginsky, N. M. Physicochemical mechanics and nonequilibrium chemical thermodynamics, *Entropy*, 2023, vol. 25, iss. 9. 13 p. DOI: 10.3390/e25091332

31. Arabczyk, W., Pelka, R., Wilk, B., Lendzion-Bieluń, Z. Kinetics and thermodynamics of the phase transformation in the nanocrystalline substance--gas phase system', *Crystals*, 2024, vol. 14, iss. 2. 21 p. DOI: 10.3390/cryst14020129

32. Abdulla, N. *CEAPlugins.py* [Source code]. CEA-Thermochemical-Analysis. GitHub, 2026. Available at: https://github.com/nijatabdulla/CEA-Thermochemical-Analysis/blob/main/CEAPlugins.py

Received 27.05.2026, Received in revised form 15.07.2026
Accepted date 17.08.2026, Published date 26.08.2026

ЧИСЕЛЬНИЙ АНАЛІЗ БАГАТОФАЗНИХ СЕРЕДОВИЩ У РОЗВ'ЯЗУВАЧАХ БАГАТОФАЗНОЇ ХІМІЧНОЇ РІВНОВАГИ

Ніджат Абдулла

У статті представлено критерій фазової стабільності для обробки поліморфних конденсованих частинок при високоточному моделюванні хімічної рівноваги. **Метою** статті є запобігання блокуванню поліморфів, використанню недійсних коефіцієнтів і нестабільному перемиканню фаз при мінімізації вільної енергії Гіббса, коли ідентичні за складом тверді фази мають невеликі відмінності у вільній енергії поблизу переходу тверде тіло-тверде тіло. Використовувані **методи** базуються на ідентифікації ідентичних за складом середовищ у конденсованому стані, відокремленні справжніх поліморфних сімейств від випадків фазового переходу тверде тіло-рідина та визначенні температур переходу тверде тіло-тверде тіло на основі суміжності інтервалів термохімічної бази даних за допомогою спеціальної процедури виявлення фазового переходу. Стабільний поліморф вибирається відповідно до поточної температури відносно визначеної межі, зберігаючи при цьому елементний склад та стехіометричні обмеження. Якщо температуру переходу неможливо достовірно визначити, застосовується перевірка температурної достовірності, й поліморфи, що виходять за межі діапазону, замінюються допустимими аналогами ідентичного складу. Цей шар фазової допустимості поєднується з тестом на стабільність конденсованого активного набору; це гарантує, що в рівноважному розчині залишаються лише термодинамічно стабілізуючі конденсовані фази. **Новизна** статті полягає в явній інтеграції логіки фазової стабільності поліморфів в ітерації багатофазної рівноваги горіння на основі ККТ та процедури прийняття рішень на основі активного набору. Запропонований критерій регуляризує перемикання між твердими тілами, запобігає витоку термодинамічних даних за межі дійсних поліноміальних інтервалів і покращує стійкість збіжності поблизу областей фазових меж. Еталонні випадки температурного сканування, що включають поліморфи Cr_2O_3, демонструють стабільний температурно-залежний вибір фази та узгодженість з NASA CEA на рівні властивостей із середньою відносною похибкою приблизно 0,05%. Результати показують, що явні критерії фазової стабільності забезпечують фізично узгоджену та надійну основу для моделювання поліморфних середовищ у розрахунках багатофазної хімічної рівноваги.

Ключові слова: моделювання хімічної рівноваги, поліморфні середовища, фазова стабільність, мінімізація вільної енергії Гібса, конденсовані фази, фазові переходи тверда тіло-тверде тіло, метод активного набору, термохімічна база даних, високотемпературне горіння, рівноважний розв'язувач на основі ККТ.

Ніджат Парвіз-оглі Абдулла – провідний інженер з рушійних систем, старший викладач кафедри рушійних та гідродинамічних систем, аспірант кафедри літальних апаратів і авіаційних двигунів, Національна авіаційна академія, Баку, Азербайджан.

Nijat Parviz oglu Abdulla – Principal Propulsion Systems Engineer, Senior Lecturer on Propulsion and Fluid Systems, PhD Candidate, Department of Flight Vehicles and Aviation Engines, National Aviation Academy, Baku, Azerbaijan,
e-mail: nijatabdulla@naa.edu.az, ORCID: 0000-0001-5608-8548